LETTERS
PUBLISHED ONLINE: 13 APRIL 2014 | DOI: 10.1038/NNANO.2014.60
nature nanotechnology

# Photoinduced doping in heterostructures of graphene and boron nitride

L. Ju[1†], J. Velasco Jr[1†], E. Huang[1], S. Kahn[1], C. Nosiglia[1], Hsin-Zon Tsai[1], W. Yang[2], T. Taniguchi[3], K. Watanabe[3], Y. Zhang[4], G. Zhang[2], M. Crommie[1,5,6], A. Zettl[1,5,6] and F. Wang[1,5,6]*

**The design of stacks of layered materials in which adjacent layers interact by van der Waals forces[1] has enabled the combination of various two-dimensional crystals with different electrical, optical and mechanical properties as well as the emergence of novel physical phenomena and device functionality[2–8]. Here, we report photoinduced doping in van der Waals heterostructures consisting of graphene and boron nitride layers. It enables flexible and repeatable writing and erasing of charge doping in graphene with visible light. We demonstrate that this photoinduced doping maintains the high carrier mobility of the graphene/boron nitride heterostructure, thus resembling the modulation doping technique used in semiconductor heterojunctions, and can be used to generate spatially varying doping profiles such as p–n junctions. We show that this photoinduced doping arises from microscopically coupled optical and electrical responses of graphene/boron nitride heterostructures, including optical excitation of defect transitions in boron nitride, electrical transport in graphene, and charge transfer between boron nitride and graphene.**

Recent scanning probe and electrical transport studies have revealed moiré patterns[2–4], new Dirac points[5] and the Hofstadter butterfly[6–8] in graphene/boron nitride (G/BN) heterostructures, hence convincingly demonstrating that the interaction between the constituents of van der Waals heterostructures (VDHs) plays a key role in their properties. Light–matter interactions in VDHs can also exhibit new phenomena arising from the coupling between the layered constituents. A recent work exploited the strong optical absorption of $WS_2$ and the tunability of graphene electrodes to engineer graphene/$WS_2$/graphene heterostructures for flexible photovoltaic devices with high quantum efficiency[9]. Here, we demonstrate an emerging optoelectronic response in G/BN heterostructures, where patterned doping of graphene can be controllably written and erased through optical excitation of BN. This photoinduced doping is analogous to the modulation doping in semiconductor heterojunctions in that it preserves the remarkably high mobility of G/BN[10,11] by having the dopants separated from the conducting channel. This photoinduced 'modulation' doping in G/BN heterostructures arises from defect states in the bulk of crystalline BN flakes. It is qualitatively different from photoinduced effects previously observed in graphene on $SiO_2$ (G/$SiO_2$), which originates from interfacial charge traps in the amorphous oxide[12,13]. Moreover, compared with G/$SiO_2$ devices, the photodoping response in G/BN is more than 1,000 times stronger. It leads to an electron mobility more than an order of magnitude higher and it has superior stability and reversibility. These unique features of photodoping in G/BN could enable novel high-quality graphene electronic devices using a photoresist-free photolithography, where the BN substrate itself acts as the photosensitive medium.

Graphene charge transport in the G/BN heterostructure can be modified upon illumination even with an incandescent lamp, as we show in Fig. 1. We monitored the graphene resistance $R$ while sweeping the bottom gate voltage $V_g$ with different optical excitation conditions. The graphene resistance shows a sharp peak at the charge neutral point (CNP) with $V_g \approx 0$ V and has little hysteresis in the absence of light exposure (Fig. 1a), similar to that observed in many graphene field-effect-transistor devices[10,11,14,15]. The transport behaviour becomes completely different, however, when the device is exposed to moderate optical illumination.

In Fig. 1b, we plot the gate-dependent graphene resistance when the device is under illumination from an incandescent lamp. $V_g$ is swept from 70 V to −70 V and then back to 70 V. We observe that $R$ initially increases until it reaches the CNP at $V_g = 0$ V. Subsequently, $R$ remains constant as $V_g$ sweeps to negative voltages, as if the gating is not working. This is in striking contrast to the behaviour without light illumination (Fig. 1a). When the $V_g$ sweep is reversed, $R$ drops quickly as if the reversal point (rather than $V_g = 0$) is the CNP.

To further investigate this intriguing photoinduced response, we measured $R(V_g)$ while alternately switching the light off and on as $V_g$ was swept from 20 V to −50 V at a constant rate of 0.05 V $s^{-1}$ (Fig. 1c). We observed conventional $R(V_g)$ behaviour when the light was off (for $V_g = 20$ V to −5 V), and $R$ increased quickly and became pinned at the CNP value whenever light was switched on. Once the light was switched off, $R$ decreased from the CNP value with more negative $V_g$.

Although the photoinduced responses under different illumination conditions seem quite complicated, they can be understood with a very simple phenomenological model, as illustrated in Fig. 1d,e. In this model, visible light induces a positive charge distribution in BN that completely screens the negative $V_g$, and the positive charges in BN are fixed when the light is switched off. This model explains qualitatively all of our experimental observations: the backgate is screened and graphene is pinned at the CNP with the light on and at negative $V_g$, and this $V_g$ sets the CNP when the light is off or $V_g$ becomes less negative. When the $V_g$ is removed, it results in a stable n-type doping in graphene. Because the positive dopants (in BN) are remote from the n-type conducting channel (in graphene), this is analogous to the modulation doping first developed for high-quality semiconductor heterojunctions[16,17], where dopants are separated

[1]Department of Physics, University of California, Berkeley, California 94720, USA, [2]Beijing National Laboratory for Condensed Matter Physics and Institute of Physics, Chinese Academy of Sciences, Beijing 100190, China, [3]National Institute for Materials Science, 1-1 Namiki, Tsukuba, 305-0044, Japan, [4]State Key Laboratory of Surface Physics and Department of Physics, Fudan University, Shanghai 200433, China, [5]Materials Sciences Division, Lawrence Berkeley National Laboratory, Berkeley, California 94720, USA, [6]Kavli Energy NanoSciences Institute at the University of California, Berkeley and the Lawrence Berkeley National Laboratory, Berkeley, California, 94720, USA. †These authors contributed equally to this work. *e-mail: fengwang76@berkeley.edu

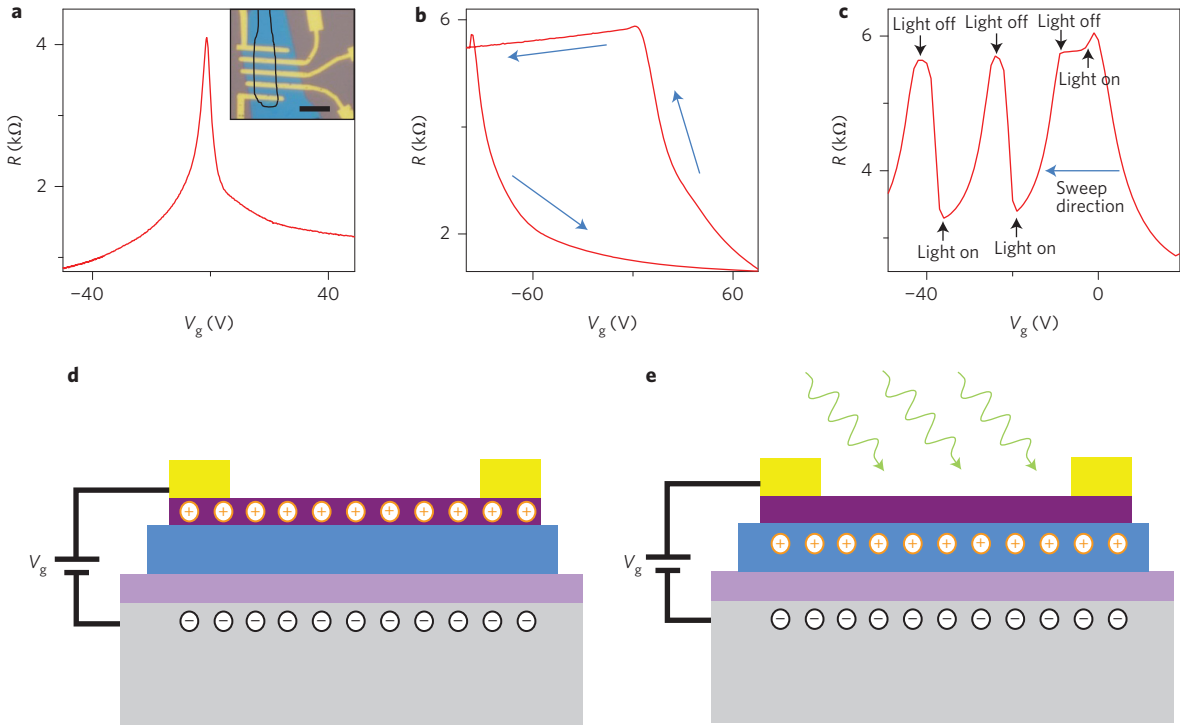


**Figure 1 | Experimental observation of photoinduced modulation doping effect in G/BN heterostructures. a**, Representative $R(V_g)$ data in a G/BN device showing a sharp resistance peak at $V_g = 0$ without light exposure. Inset: Optical micrograph of device, with graphene (outlined by the solid line) on a BN flake (blue, 18 nm thick) and contacted by chrome/gold electrodes. Scale bar, 8 μm. **b**, $R(V_g)$ trace as $V_g$ sweeps from 70 V to −70 V and then back to 70 V with the device exposed to light. Light illumination changed the gating behaviour in the graphene, with negative gating becoming ineffective and the graphene resistance remaining at the CNP value. The BN flake here and in **c** is ~100 nm thick. **c**, $R(V_g)$ trace when $V_g$ sweeps from 20 V to −50 V and the light illumination is alternately switched on and off. Graphene resistance is pinned at CNP value whenever light is switched on at negative $V_g$ and shows normal gating behaviour when light is switched off. **d**,**e**, Charge distribution in the G/BN device when light (green arrows) is switched off (**d**) and on (**e**). Positive charges accumulate in BN under light illumination at negative $V_g$, which effectively screens the backgate and keeps graphene at the CNP. Yellow, Cr/Au; purple, graphene; blue, BN; violet, $SiO_2$; grey, Si.

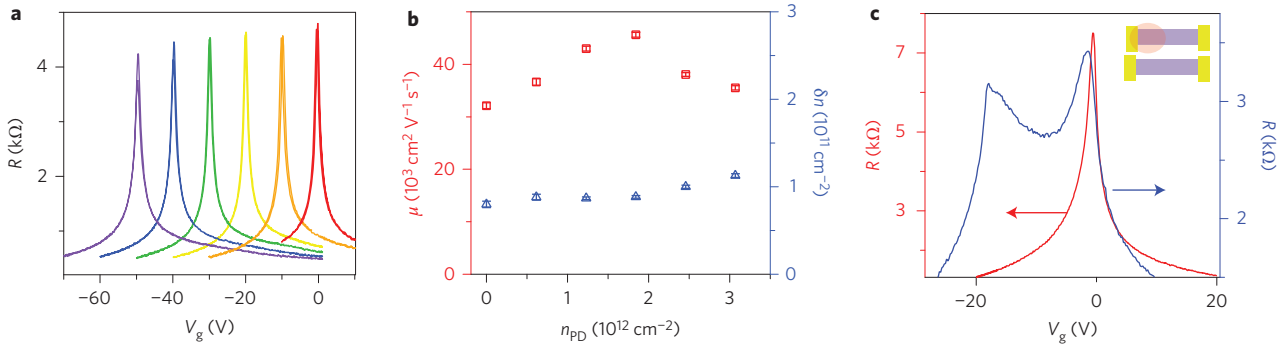


**Figure 2 | Transport characteristics of G/BN after photoinduced modulation doping. a**, $R(V_g)$ traces displaying high-mobility charge transport in G/BN devices with photoinduced modulation doping. Red trace: Behaviour of a pristine sample. The other traces were acquired after photodoping, with the graphene CNP set at $V_g = -10$, −20, −30, −40 and −50 V, respectively (from right to left). The BN flake is ~80 nm thick. **b**, Quantitative determination of electron mobility $\mu$ (squares, left axis) and charge density fluctuation $\delta n$ at the CNP (triangles, right axis) from $R(V_g)$ traces in **a**, at different photoinduced doping density $n_{PD}$. Error bars represent ±1 s.d. **c**, Generation and erasure of a p-n junction in a G/BN heterostructure with light. Inhomogeneous photodoping can be established by illuminating part of the G/BN device with light at $V_g = -20$ V (inset), which results in an $R(V_g)$ response typical of a graphene p-n junction (blue trace). Subsequent exposure of the device to light at $V_g = 0$ V erases the inhomogeneous doping and recovers the $R(V_g)$ response of pristine graphene (red trace).

from the conducting channel to prevent charge scattering. Although the photoinduced 'modulation' doping in G/BN is not permanent, we found it can last for many days at room temperature when the device is kept in a dark environment. Furthermore, it can be erased easily within minutes with light illumination at an intensity of ~10 μW μm$^{-2}$. Further measurements show that a p-type doping can also be induced in G/BN by optical excitation at a positive $V_g$, but the dynamics is orders of magnitude slower. We have measured 27 G/BN samples, and all exhibit the photodoping effect. However, the exact dynamics of photodoping can vary significantly depending on both the BN flake thickness and the batch of parent BN crystals.

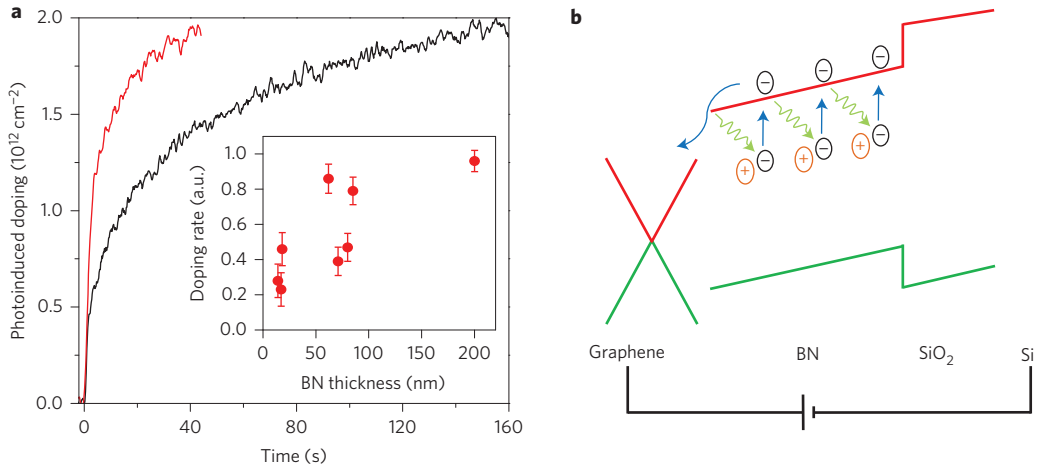


**Figure 3 | Dynamics and origin of photoinduced modulation doping effect. a**, Photoinduced doping density as a function of time in two devices under the same illumination condition and gating electrical field. Black and red traces correspond to BN flake thicknesses of 20 nm and 110 nm, respectively. Evidently, the rate of photodoping is significantly higher in the G/BN device with a thicker BN flake. Inset: Photodoping rate in more samples, showing that the rate increases systematically with BN thickness, although it fluctuates significantly from sample to sample. The error bars are defined by the error in determining $\Delta V_g$, which is within $\pm$0.2 V (see Supplementary Section 4 for details). **b**, Schematics of the band structure of the graphene/BN heterostructure and illustration of the photodoping mechanism, where optical excitation first excites electrons from defects in BN. Red (green) lines represent the conduction (valence) band. The excited electrons move into the graphene under the applied gate electrical field, and the positively charged defects lead to modulation doping in the graphene when the light and $V_g$ is off.

Photoinduced modulation doping offers two distinct advantages for novel graphene electronic and optoelectronic devices. First, optical illumination provides incredible flexibility for control of doping: different doping concentrations and patterns can be written using light, and they can be generated and erased at will. Second, the doping mechanism preserves the remarkably high mobility typical of G/BN.

Figure 2a,b shows the excellent transport properties of graphene with photoinduced modulation doping. We control the doping level by exposing the device to light at fixed $V_g$ until the resistance stabilizes, and then take an $R(V_g)$ scan with the light off. We used $V_g$ set points at 0 (before doping), $-10$, $-20$, $-30$, $-40$ and $-50$ V and plot the resulting $R(V_g)$ traces in Fig. 2a. The photoinduced doping leads to a shift of the CNP to the $V_g$ set points, corresponding to an n-doping concentration. Remarkably, the peaks of all $R(V_g)$ plots remain as sharp as the pristine sample. This is in striking contrast to doping induced by adsorbed atoms, where a significant increase of $R(V_g)$ peak width accompanies higher doping concentrations[18–20]. Figure 2b quantifies the charge transport properties by plotting the charge density fluctuations $\delta n$ and mobilities $\mu$ close to the CNP for different photoinduced doping concentrations (Supplementary Fig. 1). Evidently, the photoinduced doping preserves the excellent electrical transport properties of G/BN. The electron mobility $\mu$ remains almost constant over the entire range of doping concentrations. $\delta n$ exhibits similar behaviour and increases only marginally as the doping level increases to $3 \times 10^{12}$ cm$^{-2}$.

Figure 2c demonstrates the flexibility of photoinduced doping to optically control the doping profile of G/BN. We created a high-quality graphene p–n junction by exposing one region of the sample to light with $V_g$ set at $-20$ V (Fig. 2c, inset). The resulting $R(V_g)$ trace taken with the light off is shown in Fig. 2c (blue line). Two distinct peaks are observed, which have similar heights and are separated by $-16$ V. This transport behaviour is characteristic of a graphene p–n junction[21–23]. This photoinduced doping can last for days if the device is kept in a dark environment, or it can be erased by exposing the sample to white light with $V_g = 0$ V. The erasure process usually requires 50 times higher illumination dosage (power density $\times$ exposure time) than the doping process. The red trace in Fig. 2c shows the $R(V_g)$ curve after the erasing process; it has a single sharp peak centred at $V_g = 0$ V as in the pristine device.

Combining the photoinduced modulation doping with photolithography techniques can enable scalable fabrication of high-mobility graphene devices with arbitrary doping pattern. This fabrication scheme does not require any photoresist because G/BN itself is the photosensitive medium. Also, the device is rewritable by controlling light illumination. It offers distinct advantages over alternative techniques used to create graphene p–n junctions that require nontrivial multi-step fabrication processes that reduce sample quality[21,22] and/or generate irreversible doping[24].

We next studied the microscopic processes responsible for photoinduced modulation doping in G/BN. First, we needed to identify the electronic states being excited by photons that lead to photodoping effects. The initial optical excitation might take place at the G-BN interface (by exciting graphene or special interface states[12,13]) or inside the BN. These two cases can be differentiated by examining the photodoping dynamics with different BN thicknesses, because the photodoping rate will have a positive correlation with BN thickness if electronic states in BN are excited, and it will be independent of BN thickness if interface states are excited. Figure 3a shows the experimental data for G/BN heterostructures with 20 nm and 110 nm BN flakes. These two BN flakes were exfoliated from the same scotch tape to ensure that they had the same physical properties. At $t = 0$ s we set $V_g = -30$ V for the 20 nm BN sample ($-40$ V for the 110 nm BN sample to ensure the same doping density) and switched on the light. From Fig. 3a we can see that the dynamic resistance increase (or photodoping rate) is much faster in the 110 nm BN sample than in the 20 nm BN sample under the same illumination condition. Results for more samples are plotted in the inset of Fig. 3a. We observe a systematic increase in photodoping rate in thicker BN flakes, although a significant variation of doping rate is observed. Our results suggest that optical excitation of electronic states inside BN initializes the photoinduced doping in G/BN heterostructures. The typical light power density we used was 0.1–1 $\mu$W $\mu$m$^{-2}$, which is three orders of magnitude lower than that required to observe photodoping originating from interfacial charge traps in $SiO_2$[12,13].

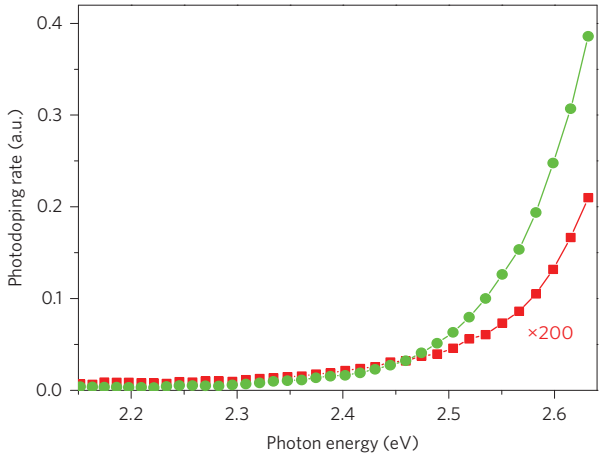


**Figure 4 | Optical spectrum of defect states in h-BN.** Photodoping rate as a function of photon energy for donor (acceptor) states is extracted by applying a negative (positive) $V_g$. The green trace shows that the photodoping rate (and therefore the absorption cross-section) from donor states keeps increasing in the experimental spectral range (up to 2.6 eV). A similar trend is observed for acceptor-like states (red trace), but this photodoping rate is about two orders of magnitude lower. These spectral dependences suggest deep donor and acceptor defect levels close to the middle of the BN bandgap. The BN flake is ~60 nm thick.

In the past, BN was always considered to be an inert substrate because it has a bandgap of 6.4 eV (ref. 25). Accordingly, it is quite surprising that the photoinduced doping in G/BN originates from optical excitation of electronic states in BN. Obviously, the visible photons used in the experiment cannot excite the bandgap transitions, but they can excite defect states in BN. In Fig. 3b we illustrate a physical picture of the photoinduced doping in G/BN starting with defect states in BN. Graphene is initially hole-doped at a negative $V_g$ in the dark, and an electric field emanates from graphene to silicon. Upon optical illumination, electrons of donor-like defects in BN are excited by photons to the conduction band. These excited electrons can be mobile and move towards the graphene, following the existing electrical field, and then enter the graphene. The ionized defects are positively charged and localized in the BN, and they effectively screen the backgate. The process continues until the electric field in the BN vanishes and graphene becomes charge neutral, as we observed experimentally. Because the ionized defects are within the BN flake, which are on average tens of nanometres away from the graphene, they introduce minimum extra scattering in the graphene[26]. Additionally, correlations between these charged defects can reduce the scattering even more[27]. Negatively charged defects can also be generated in BN if optical excitation excites acceptor-like defects in BN at a positive $V_g$. However, the process is much slower in our experiment, presumably due to a much lower concentration of acceptor-like defects in BN.

With this microscopic understanding, we can employ the photoinduced doping in G/BN as a tool to study the nature of the BN defect states. The optical absorption cross-section of defect states in BN is proportional to the generation rate of ionized defects, which can be measured sensitively through their effect on graphene electrical transport (Supplementary Fig. 5). Moreover, we can probe selectively the donor-like defects and acceptor-like defects by setting $V_g$ to be negative and positive, respectively. Figure 4 shows the photodoping rate for acceptor-like defects (red trace) and donor-like defects (green trace) as a function of photon energy. We found that photodoping rate, which is proportional to the optical absorption of the defect states, varies with defect type and excitation energy. For donor-like states, we found that the absorption cross-section keeps increasing in the experimental spectral range (up to 2.6 eV). A similar trend is observed for acceptor-like states, but the photodoping rate is approximately two orders of magnitude lower. These spectral dependences suggest deep donor and acceptor defect levels close to the middle of the BN bandgap. Previous theoretical work has found that the dominating donor and acceptor absorption resonances are from a nitrogen vacancy at 2.8 eV and a carbon impurity (substituting a nitrogen atom) at 2.6 eV (ref. 28). These resonances are slightly beyond our experimental spectral range, but are consistent with the observed strong rise below 2.6 eV. A greater spectrum range in the higher photon energy regime will be necessary to directly probe the absorption resonances from the defect levels.

In summary, we have observed a strong photoinduced modulation doping effect in G/BN heterostructures and have provided a microscopic description of its origin. This effect can enable flexible fabrication of graphene devices through controlled light exposure as in photolithography. Moreover, it allows for repeatable writing and erasing of the doping features and preserves the very high mobility of G/BN. This new and simple technique of creating inhomogeneous doping in a high-mobility graphene device opens the door to novel scientific studies and applications.

## Methods

Most samples were fabricated with the transfer technique developed by Zomer and colleagues[11] and using standard electron-beam lithography. We used an h-BN thickness of 10–110 nm and a $SiO_2$ thickness of 285 nm as the dielectrics for electrostatic gating. Monolayer graphene exfoliated from Kish graphite was deposited onto a methyl methacrylate (MMA) polymer and transferred to exfoliated hexagonal boron nitride (h-BN) sitting on a $SiO_2$/Si wafer. We used a standard a.c. current biased lock-in technique with 15 nA at 97.13 Hz in a cryostat at 77 K and under a vacuum of $1 \times 10^{-5}$ torr. A fibre-based supercontinuum laser was guided into the cryostat through an optical window and a different wavelength was obtained through diffraction from a grating. We also investigated several devices using epitaxially grown graphene on BN flakes[29], which exhibited similar behaviour.

Received 21 November 2013; accepted 21 February 2014; published online 13 April 2014

## References

1. Geim, A. K. & Grigorieva, I. V. Van der Waals heterostructures. *Nature* **499,** 419–425 (2013).
2. Li, G. *et al.* Observation of Van Hove singularities in twisted graphene layers. *Nature Phys.* **6,** 109–113 (2010).
3. Xue, J. *et al.* Scanning tunnelling microscopy and spectroscopy of ultra-flat graphene on hexagonal boron nitride. *Nature Mater.* **10,** 282–285 (2011).
4. Decker, R. G. *et al.* Local electronic properties of graphene on a BN substrate via scanning tunneling microscopy. *Nano Lett.* **11,** 2291–2295 (2011).
5. Yankowitz, M. *et al.* Emergence of superlattice Dirac points in graphene on hexagonal boron nitride. *Nature Phys.* **8,** 382–386 (2012).
6. Ponomarenko, L. A. *et al.* Cloning of Dirac fermions in graphene superlattices. *Nature* **497,** 594–597 (2013).
7. Dean, C. R. *et al.* Hofstadter's butterfly and the fractal quantum Hall effect in moiré superlattices. *Nature* **497,** 598–602 (2013).
8. Hunt, B. *et al.* Massive Dirac fermions and Hofstadter butterfly in a van der Waals heterostructure. *Science* **340,** 1427–1430 (2013).
9. Britnell, L. *et al.* Strong light–matter interactions in heterostructures of atomically thin films. *Science* **340,** 1311–1314 (2013).
10. Dean, C. R. *et al.* Boron nitride substrates for high-quality graphene electronics. *Nature Nano* **5,** 722–726 (2010).
11. Zomer, P. J., Dash, S. P., Tombros, N. & van Wees, B. J. A transfer technique for high mobility graphene devices on commercially available hexagonal boron nitride. *Appl. Phys. Lett.* **99,** 232104 (2011).
12. Kim, Y. D. *et al.* Focused-laser-enabled p–n junctions in graphene field-effect transistors. *ACS Nano* **7,** 5850–5857 (2013).
13. Tiberj, A. *et al.* Reversible optical doping of graphene. *Sci. Rep.* **3,** 2355 (2013).
14. Novoselov, K. S. *et al.* Electric field effect in atomically thin carbon films. *Science* **306,** 666–669 (2004).
15. Zhang, Y. B., Tan, Y. W., Stormer, H. L. & Kim, P. Experimental observation of the quantum Hall effect and Berry's phase in graphene. *Nature* **438,** 201–204 (2005).
16. Dingle, R., Stormer, H. L., Gossard, A. C. & Wiegmann, W. Electron mobilities in modulation-doped semiconductor heterojunction super-lattices. *Appl. Phys. Lett.* **33,** 665–667 (1978).

17. Pfeiffer, L., West, K. W., Stormer, H. L. & Baldwin, K. W. Electron mobilities exceeding $10^7$ $cm^2/V$ s in modulation-doped GaAs. *Appl. Phys. Lett.* **55,** 1888–1890 (1989).
18. Schedin, F. *et al.* Detection of individual gas molecules adsorbed on graphene. *Nature Mater.* **6,** 652–655 (2007).
19. Chen, J. H. *et al.* Charged-impurity scattering in graphene. *Nature Phys.* **4,** 377–381 (2008).
20. Pi, K. *et al.* Electronic doping and scattering by transition metals on graphene. *Phys. Rev. B* **80,** 075406 (2009).
21. Huard, B. *et al.* Transport measurements across a tunable potential barrier in graphene. *Phys. Rev. Lett.* **98,** 236803 (2007).
22. Williams, J. R., DiCarlo, L. & Marcus, C. M. Quantum Hall effect in a gate-controlled p–n junction of graphene. *Science* **317,** 638–641 (2007).
23. Ozyilmaz, B. *et al.* Electronic transport and quantum Hall effect in bipolar graphene p–n–p junctions. *Phys. Rev. Lett.* **99,** 166804 (2007).
24. Lohmann, T., von Klitzing, K. & Smet, J. H. Four-terminal magneto-transport in graphene p–n junctions created by spatially selective doping. *Nano Lett.* **9,** 1973–1979 (2009).
25. Museur, L. *et al.* Exciton optical transitions in a hexagonal boron nitride single crystal. *Phys. Status Solidi RRL* **5,** 214–216 (2011).
26. Hwang, E. H., Adam, S. & Das Sarma, S. Carrier transport in two-dimensional graphene layers. *Phys. Rev. Lett.* **98,** 186806 (2007).
27. Yan, J. & Fuhrer, M. S. Correlated charged impurity scattering in graphene. *Phys. Rev. Lett.* **107,** 206601 (2011).
28. Attaccalite, C., Bockstedte, M., Marini, A., Rubio, A. & Wirtz, L. Coupling of excitons and defect states in boron-nitride nanostructures. *Phys. Rev. B* **83,** 144115 (2011).
29. Yang, W. *et al.* Epitaxial growth of single-domain graphene on hexagonal boron nitride. *Nature Mater.* **12,** 792–797 (2013).

## Acknowledgements

The authors thank P. Jarillo-Herrero and N. Gabor for stimulating discussions and B. Standley for help with data acquisition software. Graphene synthesis, device fabrication and optical measurements were supported by the Office of Naval Research (award N00014-13-1-0464). Electrical measurements and theoretical analysis of this work were mainly supported by the Office of Basic Energy Science, Department of Energy (contract no. DE-SC0003949, Early Career Award; DE-AC02-05CH11231, Materials Science Division). F.W. acknowledges support from a David and Lucile Packard fellowship. J.V.J. acknowledges support from the UC President's Postdoctoral fellowship.

## Author contributions

F.W. and L.J. conceived the experiment. L.J. and J.V.J. carried out optical and electronic measurements. J.V.J., E.H., S.K., C.N., H.T and W.Y. contributed to sample fabrication, K.W. and T.T. synthesized the h-BN samples, F.W., J.V.J. and L.J. performed data analysis and theoretical analysis. F.W., L.J. and J.V.J. co-wrote the manuscript. All authors discussed the results and commented on the paper.

## Additional information

Supplementary information is available in the online version of the paper. Reprints and permissions information is available online at www.nature.com/reprints. Correspondence and requests for materials should be addressed to F.W.

## Competing financial interests

The authors declare no competing financial interests.